Available online at www.sciencedirect.com
ScienceDirect
Journal of Colloid and Interface Science 316 (2007) 442–450
JOURNAL OF Colloid and Interface Science
www.elsevier.com/locate/jcis

Effect of microemulsion variables on copper oxide nanoparticle uptake by AOT microemulsions

Nashaat N. Nassar, Maen M. Husein *

Department of Chemical and Petroleum Engineering, University of Calgary, Calgary, AB, T2N 1N4, Canada

Received 20 April 2007; accepted 21 August 2007

Available online 28 August 2007

Abstract

Ultradispersed metal oxide nanoparticles have applications as heterogeneous catalysts for organic reactions. Their catalytic activity depends primarily on their surface area, which in turn, is dictated by their size, colloidal concentration and stability. This work presents a microemulsion approach for in situ preparation of ultradispersed copper oxide nanoparticles and discusses the effect of different microemulsion variables on their stability and highest possible time-invariant colloidal concentration (nanoparticle uptake). In addition, a model which describes the effect of the relevant variables on the nanoparticle uptake is evaluated. The preparation technique involved solubilizing $CuCl_2$ in single microemulsions followed by direct addition of NaOH. Upon addition of NaOH, copper hydroxide nanoparticles stabilized in the water pools formed in addition to a bulk copper hydroxide precipitate at the bottom. The copper hydroxide nanoparticles transformed with time into copper oxide. After reaching a time-independent concentration, mixing had limited effect on the nanoparticle uptake and particle size. Particle size increased with increasing the surfactant concentration, concentration of the precursor salt, and water to surfactant mol ratio; while the nanoparticle uptake increased linearly with the surfactant concentration, displayed an optimum with R and a power function with the concentration of the precursor salt. Surface areas per gram of nanoparticles were much higher than literature values. Even though lower area per gram of nanoparticles was obtained at higher uptake, higher surface area per unit volume of the reverse micellar system was attained. A model based on water uptake by Wisor type II microemulsions, and previously used to describe iron oxide nanoparticle uptake by the same microemulsions, agreed well with the experimental results.
© 2007 Published by Elsevier Inc.

Keywords: Nanoparticle; Copper oxide; Microemulsion; Surfactant; Catalyst; Surface area; Uptake; Model

1. Introduction

Formation of well-dispersed colloidal nanoparticle catalysts is crucial for heterogeneous catalysis in organic media [1–12]. However, maintaining stable dispersion of the particles is a challenging issue, since these particles tend to agglomerate with time in order to reduce the high surface energy [13]. One approach of minimizing particle agglomeration is to prepare the catalyst in situ. For example, very high reaction rates were attained when in situ prepared ultradispersed catalysts were employed for hydrocracking [1,2], coprocessing [4], and coal liquefaction [12]. In these investigations organometallic precursors were dissolved in the organic media to ensure intimate dispersion, then the catalyst was prepared in situ by thermal decomposition of the corresponding precursor. Water-in-oil (w/o) microemulsions, or reverse micelles, serve as an alternative in situ preparation technique for ultradispersed nanoparticle catalysts starting from their water soluble precursors [1–4]. It offers an easy control over particle size, produces highly dispersed nanoparticles in organic phases, and protect these particles from agglomeration by virtue of the surfactant protective layer. In fact, it was found that (w/o) microemulsion-prepared nanoparticle catalysts exhibited smaller particle sizes and showed higher catalytic activity compared with the ones prepared by conventional techniques [8,9,14]. In general, high catalyst activity hinges on maintaining high accessible catalyst surface area. For ultradispersed catalysts, high accessible area can be attained by minimizing particle size and maximizing particle colloidal concentration. The condition of high colloidal concentration, in particular, poses a challenge for microemulsion systems, since

* Corresponding author.
E-mail address: maen.husein@ucalgary.ca (M.M. Husein).

0021-9797/$ – see front matter © 2007 Published by Elsevier Inc.
doi:10.1016/j.jcis.2007.08.044

they inherently suffer from low solubilization/stabilization capacities of the different species [15,16].

In a previous work, we studied the in situ formation of iron oxide nanoparticles in single AOT/water/isooctane microemulsions at high loading of precursor materials [17]. The effect of operating and microemulsion variables on the maximum possible time-independent nanoparticle concentration, nanoparticle uptake, was evaluated [17]. The current work explores the conditions at which the highest uptake of stable colloidal copper oxide nanoparticles can be attained. In addition, the work tests the applicability of our previous model [17] to the uptake of copper oxide and provides more physical insight to the model parameters. Copper oxide is employed as ultradispersed catalysts for heavy oil upgrading [1]. In addition, copper oxide nanoparticles have application in nanofluids, where high concentration of dispersed nanoparticle is invincible for achieving high thermal conductivity of the base fluid [18–20].

2. Experimental

2.1. Chemicals

The following chemicals were used: AOT, dioctylsulfosuccinate sodium salt (98%, Sigma–Aldrich Fine Chemical, ON) as the surfactant; isooctane (HPLC grade, Fisher scientific, ON) as the oil phase; copper(II) chloride (99%, ACROS, NJ) as the precursor salt; and sodium hydroxide (5.0 N, Alfa Aesar, ON) as the precipitating agent. All chemicals were used without further purification.

2.2. Nanoparticle synthesis

The colloidal copper oxide nanoparticles were prepared in situ by exposing AOT/water/isooctane microemulsions to $CuCl_2$ precursor followed by addition of NaOH at a later stage [17]. All the experiments, except the ones used to study the effect of mixing time, were performed by mixing 20 ml volume of AOT microemulsions with a specified amount of $CuCl_2$ until it completely dissolves, unless otherwise noted. A stoichiometric amount of NaOH was then added to the microemulsions and the system was left to mix for 3 h at 300 rpm and 25 °C. For the samples used to study the effect of mixing time, 40 ml volume of the microemulsion was used instead, and the samples were left to mix for 6 h.

Stock AOT microemulsions were prepared by adding AOT and distilled water to a volumetric flask and completing the volume to the mark with isooctane. Aqueous NaOH solution was accounted for in the calculation of the mol ratio of water to surfactant, R. A change in R was obtained by adding distilled water to the microemulsions before introducing any reactant. All microemulsions were freshly prepared and optically clear before introducing $CuCl_2$ powder. A complete transparent greenish solution was obtained after dissolving the $CuCl_2$. When NaOH was added to the system, the solution became cloudy. A complete transparent bluish solution resulted after shaking for 1 min. The system was left to mix for 3 h after the addition of NaOH, unless otherwise noted, and excess bluish/blackish precipitate of copper oxide formed at the bottom in all the samples. Volumes of 5 ml were collected from the experimental samples after mixing for certain times, and filtered out using Fisher Brand 0.45 μm microfilters (Cole Parmer, ON). Clear samples were obtained after filtration. The presence of colloidal copper oxide nanoparticles was confirmed using the UV–vis spectroscopy (Nicolet Evolution 100, ThermoInstruments Canada Inc., ON). Microemulsions identical to those involved in the experiments were used as blank. A range of wavelength between 250 and 450 nm was covered. The nanoparticle uptake, the molar concentration of the colloidal copper oxide nanoparticles, was determined using inductive coupled plasma (ICP) (IRIS Intrepid II XDL ThermoInstruments Canada Inc., ON). A standard containing 5 ppm was prepared by diluting 80 ppm Cu stock standard in the form of copper nanoparticles with PermiSolv™ ICP solvent (CONOSTAN Oil Analysis Standards, OK). The copper oxide nanoparticle stock standard was prepared by dissolving 2 mg $CuCl_2$ in 200 mM AOT microemulsions followed by addition of a stoichiometric amount of NaOH. During the standard preparation no bulk precipitate formed. Volumes of the filtered experimental samples were diluted with PremiSolv™ to concentrations between 2 to 5 ppm. Three replicates were prepared for some samples, and the 95% confidence intervals were calculated and presented in the figures.

Around 20 drops of the filtered sample were diluted with 2 ml of isooctane, and mixed for 1 min using vortex mixer. One drop of the isooctane solution was deposited on a copper grid covered with holey carbon film and was left to evaporate for 24 h. Photographs of the nanoparticles were collected from different locations on the copper grid using Philips Tecni TEM (voltage of 200 kV) equipped with gatan imaging filter (GIF) and a slow scan CCD camera.

3. Results and discussion

3.1. Effect of mixing time

Effect of mixing time was studied by collecting data on nanoparticle concentration from a sample that was kept mixing for 6 h at 300 rpm. The other experimental variables were 200 mM AOT, 3.0 mM $CuCl_2$, and mol ratio of water to AOT, R, of 3.0. Fig. 1 shows a decrease in the nanoparticle uptake with time followed by a plateau after around 1 h of mixing. The initial decrease in the concentration of copper species in the microemulsions is attributed to the settling time required by nanoparticles with sizes exceeding the stabilization capacity of the microemulsion system. Therefore, for the experiments to follow a 3-h mixing time was considered sufficient to ensure reaching a time-independent nanoparticle concentration. This conclusion also was supported by the UV absorption spectra presented in Fig. A1 of the Supporting material. ICP measurements performed on the samples for several months showed constant colloidal concentration of copper oxide. This result is shown in Fig. A2 of the Supporting material.

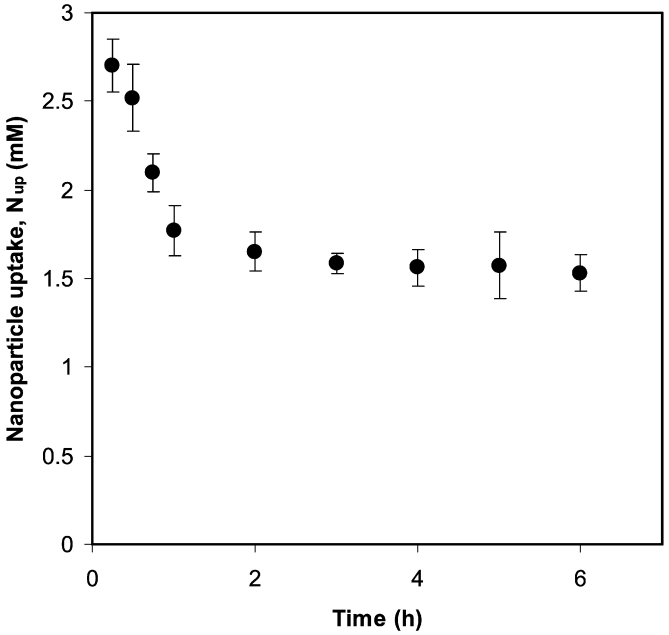

Fig. 1. Nanoparticle uptake as a function of mixing time obtained when mixing a stoichiometric amount of $CuCl_2$-containing microemulsions: {[AOT] = 200 mM, $R = 3.0$, [$CuCl_2$] = 3.0 mM} with NaOH at 300 rpm and 25 °C.

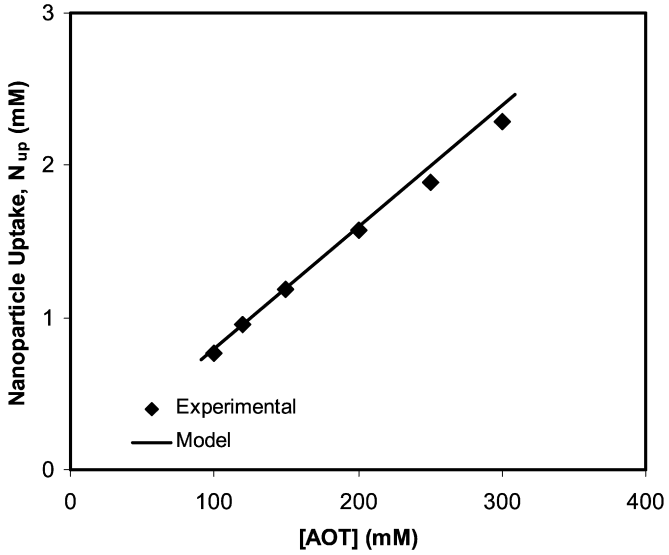

Fig. 2. Nanoparticle uptake as a function of AOT concentration obtained when mixing a stoichiometric amount of $CuCl_2$-containing microemulsions: {[$CuCl_2$] = 3.0 mM, $R = 3.0$} with NaOH for 3 h at 300 rpm.

3.2. Effect of surfactant concentration

At fixed R value, increasing surfactant concentration increases the population of reverse micelles in the organic phase [21], and hence, is expected to increase the nanoparticle uptake. The effect of increasing AOT concentration was investigated at $R = 3.0$. The concentration of $CuCl_2$ in the microemulsion was maintained constant at 3.0 mM and the stoichiometric amount of NaOH was used. Fig. 2 presents the copper oxide nanoparticle uptake as a function of surfactant concentration. The UV-absorption spectra of the colloidal copper oxide nanoparticles for 100, 200, and 300 mM AOT are depicted in Fig. 3. The TEM photographs and the corresponding particle size distribution histograms for the same samples are shown in Figs. 4a–4c.

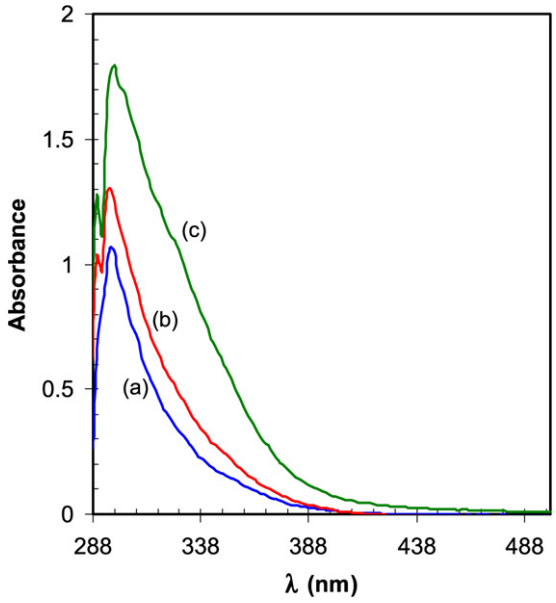

Fig. 3. UV-absorption spectra of colloidal copper oxide nanoparticles obtained when mixing a stoichiometric amount of $CuCl_2$-containing microemulsions {[$CuCl_2$] = 3.0 mM, $R = 3.0$, (a) [AOT] = 100 mM, (b) [AOT] = 200 mM, (c) [AOT] = 300 mM} with NaOH for 3 h at 300 rpm.

Fig. 2 shows that, at constant R, the nanoparticle uptake increased linearly as the surfactant concentration increased. A similar trend was reported in the literature for nanoparticle uptake by single microemulsions [22,23]. Fig. 3 shows an increase in the UV-absorption peaks as the surfactant concentration increased; consistent with the increase in the nanoparticle uptake as measured by the ICP. The TEM photographs presented in Figs. 4a–4c show an increase in the nanoparticle size as the surfactant concentration increased. A similar trend in nanoparticle size with increasing surfactant concentration was reported in the literature [22–24]. Increasing the surfactant concentration at fixed R increased the uptake due to the increase in the population of the host reverse micelles in the organic phase. Higher nanoparticle uptake increased the rate of collisions and the probability of aggregation between nanoparticle-populated reverse micelles, which led to the formation of larger particles.

Table 1 provides information on the Cu^{2+} mean occupancy number, before addition of aqueous NaOH, and the surface area provided by the stabilized nanoparticles. The mean ion occupancy number in Table 1 shows the high $CuCl_2$ loading involved in this work. The surface area per gram of the stabilized nanoparticles and the surface area per liter of the microemulsions are very relevant to ultradispersed catalysis. The surface area per gram of colloidal nanoparticles listed in Table 1 is much higher than the literature values for supported catalysts [14,25]. Even though larger surface area per gram of colloidal nanoparticles was obtained at lower surfactant concentration, larger surface area per unit volume of the microemulsion was obtained at higher uptake. A 67% increase

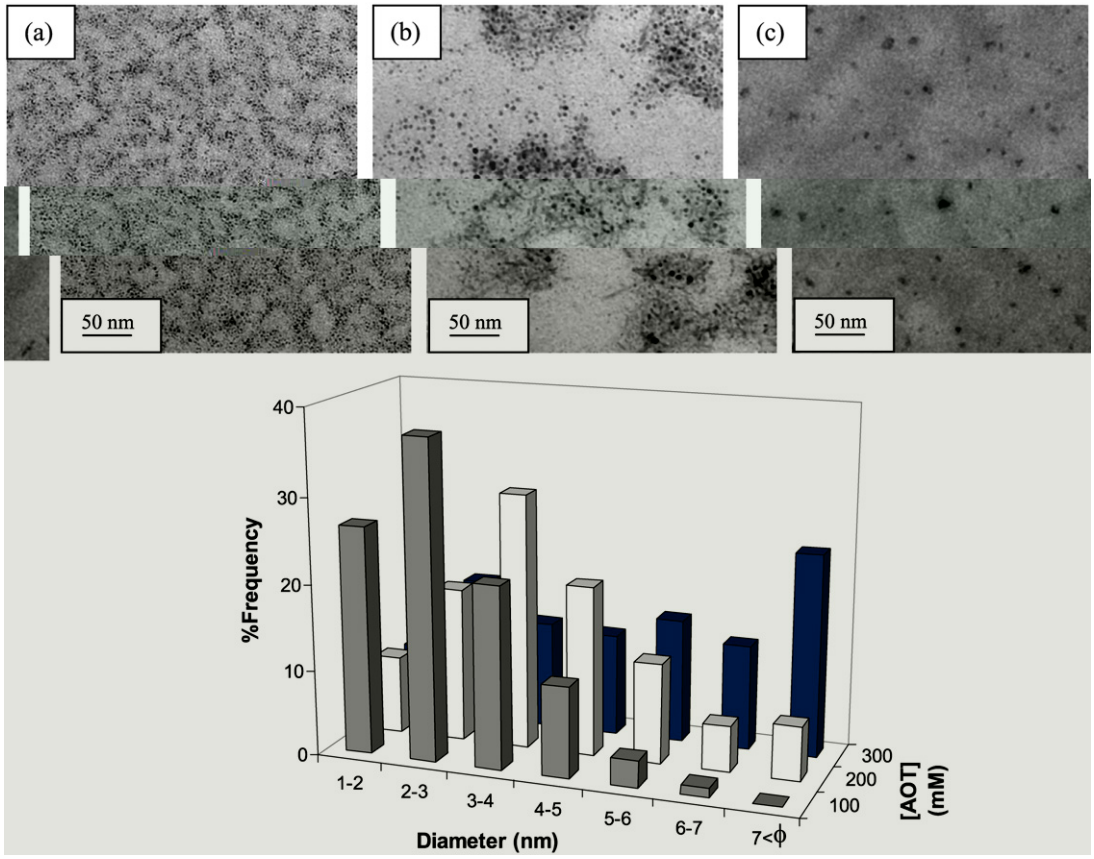

Fig. 4. TEM photographs and the corresponding particle size distribution histograms obtained when mixing a stoichiometric amount of $CuCl_2$-containing microemulsions {[$CuCl_2$] = 3.0 mM, $R = 3.0$; (a) [AOT] = 100 mM, (b) [AOT] = 200 mM, (c) [AOT] = 300 mM} with NaOH for 3 h at 300 rpm.

in the surface area per unit volume of the microemulsion was

Table 1
Mean Cu^{2+} ion occupancy number and surface area of the stabilized nanoparticles

	Before reaction		After reaction		
	Mean occupancy no. of Cu^{3+} ions[a]	Nanoparticle uptake (mM)	Number average particle diameter (nm)	Surface area/mass (m^2/g)[b]	Surface area/volume of microemulsions (m^2/l)[c]
No bulk ppt[d]	0.023	0.4			
AOT (mM)					
100	0.08	0.77	2.80	479.92	36.05
120	0.07	0.95			
150	0.06	1.19			
200	0.05	1.57	4.02	386.33	59.31
250	0.04	1.89			
300	0.04	2.28	5.01	341.34	75.99
R					
2.0	0.02	1.18	3.68	387.45	44.61
3.0	0.05	1.57	4.02	386.33	59.31
4.0	0.09	1.81			
5.0	0.15	1.81	4.49	407.94	72.02
6.5	0.27	1.57			
8.0	0.41	1.02			
$CuCl_2$ (mM)					
1.1	0.02	0.79	2.65	524.62	40.27
1.9	0.03	1.18			
3.0	0.05	1.57	4.02	386.33	59.31
3.7	0.06	1.90			
4.5	0.07	2.20			
5.5	0.07	2.44			
6.0	0.08	2.52	4.49	356.51	87.58

[a] Calculated according to Bagwe and Khilar [34,35] with *R* based on the volume of distilled water added before introducing NaOH aqueous solution.
[b] Calculated based on TEM images.
[c] Calculated based on the TEM images and nanoparticle uptake in the given volume of the microemulsions.
[d] Sample prepared at $R = 5.0$, [AOT] = 200 mM, and $CuCl_2 = 0.4$ mM.

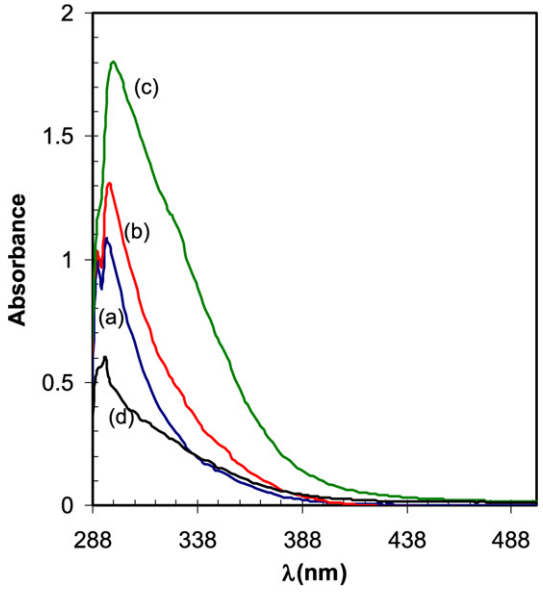

Fig. 6. UV-absorption spectra of colloidal copper oxide nanoparticles obtained when mixing a stoichiometric amount of $CuCl_2$-containing microemulsions {[$CuCl_2$] = 3.0 mM, [AOT] = 200 mM, (a) $R = 2.0$; (b) $R = 3.0$; (c) $R = 5.0$; (d) $R = 8.0$} with NaOH for 3 h at 300 rpm.

in the nanoparticle size and size distribution. The increase of the nanoparticle uptake as the water content increased can be explained as follow. At low values of *R* most of the water contributed to the bound water [21,24]. It should be noted that for $R \leqslant 2.0$ there existed undissolved $CuCl_2$ at the bottom of the vials. As *R* increased the size of reverse micelle increased and more free-water was available in the water pools to dissolve higher amounts of $CuCl_2$. For the same amounts of dissolved $CuCl_2$, $2.0 < R \leqslant 5.0$, large reverse micelles could accommodate larger particles and led to higher nanoparticle uptake. At relatively high *R*, however, the nanoparticle uptake decreased as a result of particle aggregation. As reported by Husein et al. [22,23], increasing *R* at fixed surfactant concentration reduces the interaction between the surfactant head groups and the stabilized nanoparticles. Moreover, higher water content reduces the rigidity of the surfactant protective layer and promotes particle aggregation upon collision and the formation of larger particles, which precipitate under gravity effect. The TEM images in Figs. 7a–7c show an increase in the particle size and size distribution as *R* increased. Similar trends

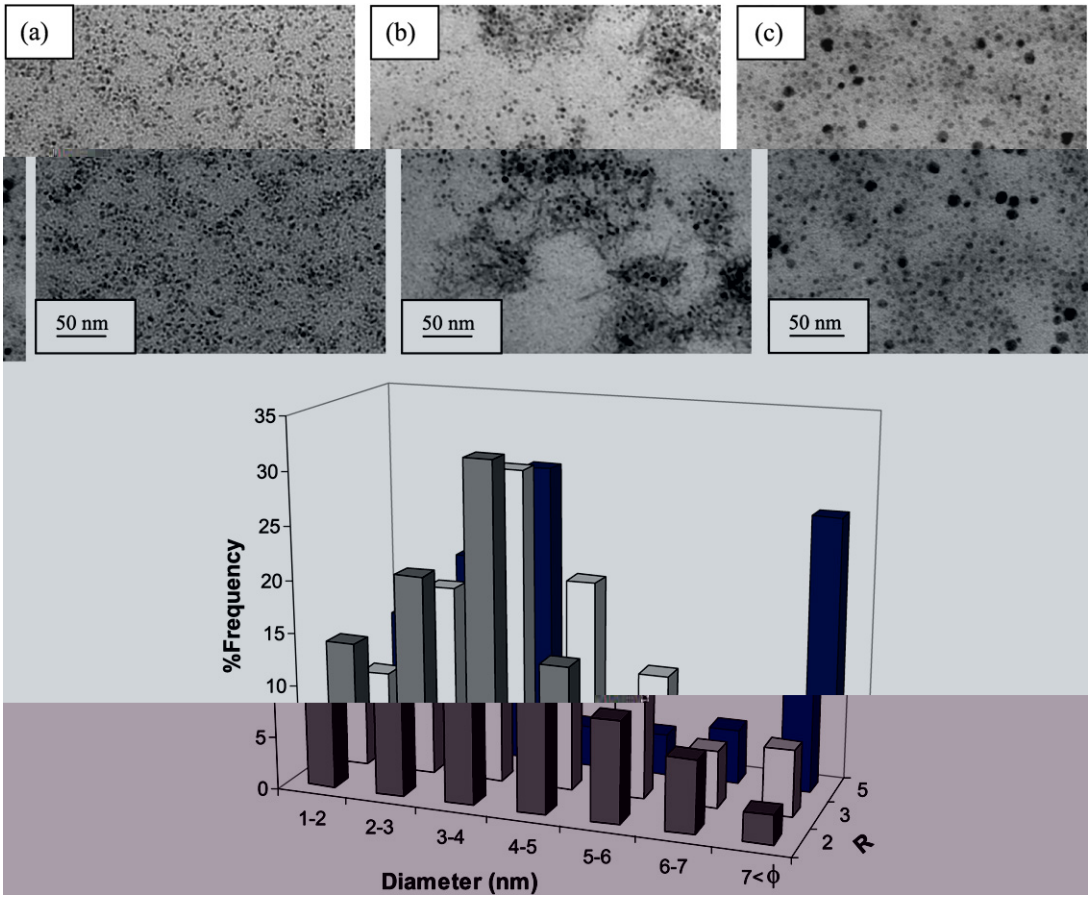

Fig. 7. TEM photographs and the corresponding particle size distribution histograms obtained when mixing a stoichiometric amount of $CuCl_2$-containing microemulsions {[$CuCl_2$] = 3.0 mM, [AOT] = 200 mM, (a) $R = 2.0$; (b) $R = 3.0$; (c) $R = 5.0$} with NaOH for 3 h at 300 rpm.

ature trend [33,34]. In order to appreciate the high reactant loading involved in this study, one should compare occupancy numbers pertaining to $R = 5.0$ and the first entry of Table 1, where no bulk precipitation occurred. A comparison between the nanoparticle uptake for $R = 3.0$ and $R = 5.0$, almost tripled, and the corresponding values of surface area per unit volume of the microemulsion, slightly increased, indicates that nanoparticle size and concentration both impact the ultradispersed catalyst surface area. At higher uptake, aggregation reduced the surface area per gram of catalyst.

3.4. Effect of precursor salt concentration

An increase in the ionic strength of the water pool induces dramatic changes in the microemulsion structure changing it from Winsor type IV over a Winsor type I to a Winsor type III to a Winsor type II [35,36]. In the current investigation we limited the effect of the ionic strength on nanoparticle size and uptake to Winsor type IV reverse micellar structure. The concentration of $CuCl_2$ in the microemulsion was increased from 1.1 to 6.0 mM, at constant mol ratio of NaOH to $CuCl_2$ of 2.0, for a surfactant concentration of 200 mM and R of 3.0.

Fig. 8 shows an increase in the nanoparticle uptake and Fig. 9 shows a corresponding increase in the size of the UV-absorption peaks as $CuCl_2$ concentration increased. This increase in the

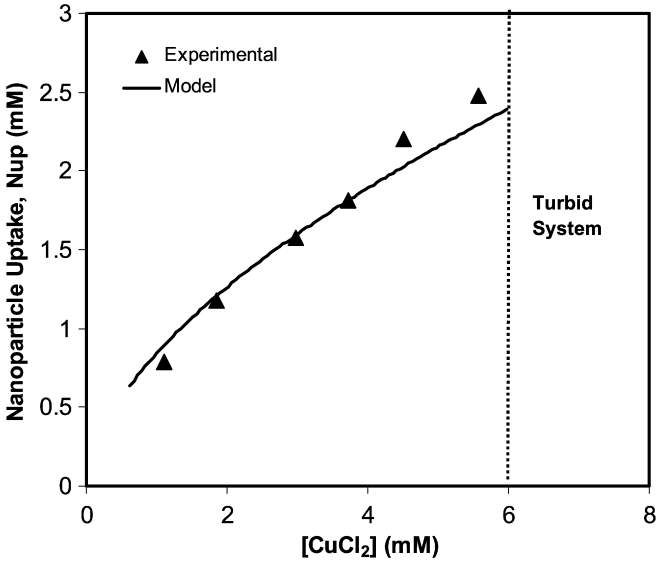

Fig. 8. Nanoparticle uptake as a function of $CuCl_2$ concentration obtained when mixing a stoichiometric amount of $CuCl_2$-containing microemulsions {$R = 3.0$, [AOT] = 200 mM} with NaOH for 3 h at 300 rpm.

nanoparticle uptake is associated with an increase in the particle size as evident from the TEM photographs of Figs. 10a–10c. The increase in the nanoparticle uptake as the concentration of $CuCl_2$ increased can be attributed to the increase of the cop-

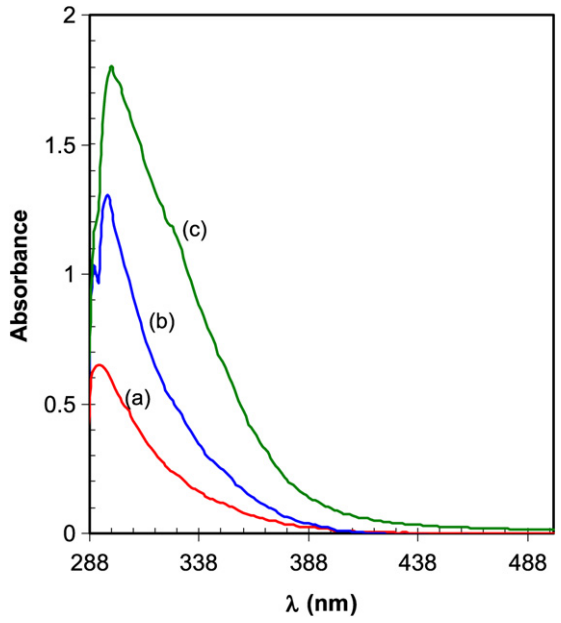

Fig. 9. UV-absorption spectra of colloidal copper oxide nanoparticles obtained when mixing a stoichiometric amount of $CuCl_2$-containing microemulsions {[AOT] = 200 mM, $R = 3.0$, (a) [$CuCl_2$] = 1.1 mM; (b) [$CuCl_2$] = 3.0 mM; (c) [$CuCl_2$] = 4.0 mM} with NaOH for 3 h at 300 rpm.

per ion occupancy number and the subsequent improvement of intramicellar nucleation and growth [21,37]. However, further increase in the $CuCl_2$ concentration resulted in the formation of a turbid system indicating a shift in Winsor equilibrium towards Winsor type II as a result of increase in ionic strength [38]. A similar trend was reported in our previous study [17], however, the system could stabilize higher amount of iron oxide nanoparticles. Again, this suggests higher interaction between the AOT head groups and the colloidal iron based nanoparticles.

Table 1 shows that a three-fold increase in $CuCl_2$ loading resulted in approximately a two-fold increase in the nanoparticle uptake and a 50% increase in the surface area per unit volume of the microemulsions. A small reduction in the surface area per gram of the nanoparticles accompanied the increase in $CuCl_2$ loading, because particle aggregation was limited by the rigid surfactant layer [22,23].

3.5. Modeling

In our previous study we have introduced a mathematical model to describe the effect of microemulsion variables on iron oxide nanoparticle uptake by AOT/water/isooctane microemulsions [17]. The model finds its roots in the empirical equations describing the linear relationship between water uptake by Winsor type II microemulsions and surfactant concentra-

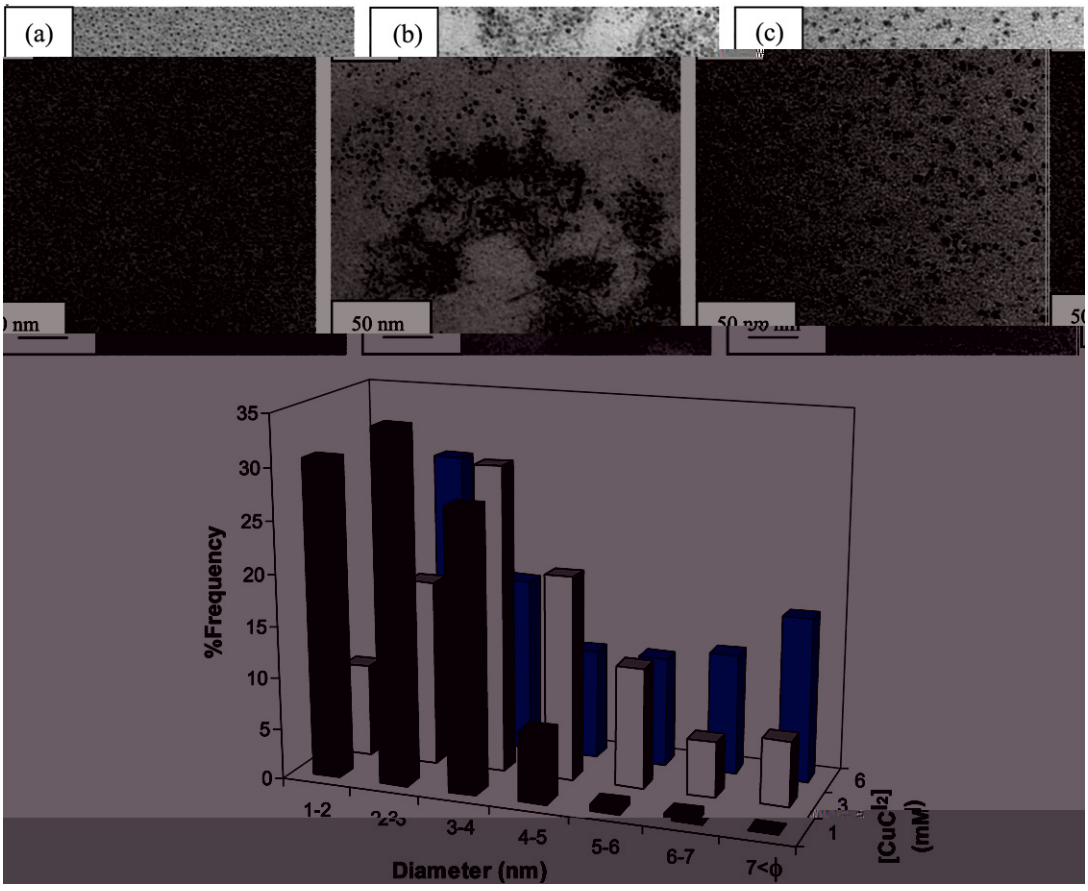

Fig. 10. TEM photographs and the corresponding particle size distribution histograms obtained when mixing a stoichiometric amount of $CuCl_2$-containing microemulsions {[AOT] = 200 mM, $R = 3.0$, (a) [$CuCl_2$] = 1.1 mM; (b) [$CuCl_2$] = 3.0 mM; (c) [$CuCl_2$] = 4.0 mM} with NaOH for 3 h at 300 rpm.

Table 2
Values of the fitted parameters for copper and iron oxide colloidal nanoparticles

Material	$\beta_1 \times 10^3$	β_2[a]	β_3
Copper oxide	2.00	0.584	−0.104
Iron oxide[a]	2.60	0.584	−0.073

[a] Ref. [17].

tion [39,40]. As evident from the experimental results, nanoparticle uptake by Winsor type IV microemulsions varied linearly with the surfactant concentration as well. Following our previous model, copper oxide nanoparticle uptake can be presented as a function of the precursor salt concentration, surfactant concentration, and R according to (E1) below. More details on the model derivation are presented in the Supporting material.

$$N_{\text{up}} = \beta_1 C^{\beta_2}\left(\beta_3 R^2 + R\right)[\text{AOT}], \tag{E1}$$

where β_1, β_2 and β_3 are fitted parameters, C is the precursor salt concentration in the microemulsion (mM), R is the water to surfactant mol ratio, and [AOT] is the surfactant concentration in the microemulsion (mM). The value of β_2 in Eq. (E1) was obtained from our previous investigation involving iron oxide nanoparticle uptake by the same microemulsions, while β_1 and β_3 were obtained from fitting Eq. (E1) to the experimental results in Figs. 2, 5 and 8. The values of β's of the current and the previous study are compared in Table 2. The model fit is excellent and the difference between the model fit and the experimental results falls within the experimental error indicated by the typical 95% confidence intervals in Fig. 1. From the above analysis, it can be concluded that β_2 is microemulsion specific, while β_1 and β_3 reflect the effect of ionic strength and amount of water on the degree of interaction between the surfactant head groups and the stabilized nanoparticles. Copper oxide has lower value of β_1 than iron oxide since the interaction between the copper oxide nanoparticles and the surfactant head groups is lower. The lower value of β_3 for copper oxide further supports the conclusion of higher interaction between iron oxide nanoparticles and the surfactant head groups. The value of the inverse of the slope of the straight line in Fig. 2 suggests that 130 mol of AOT is required to stabilized 1 mol of copper oxide nanoparticles, while in our previous study 85 mol of AOT were required to stabilize 1 mol of iron oxide [17]. The model captures the optimum value of R which corresponded to the highest copper oxide uptake. This value is smaller when compared with iron oxide uptake. This, again, supports the conclusion of higher interaction between the surfactant head groups and iron oxide nanoparticles inferred from the experiments.

4. Conclusions

This work demonstrated the use of single microemulsion approach for in situ preparation of colloidal copper oxide nanoparticles. Microemulsions are excellent media for the preparation of highly stable ultradispersed catalyst, however, they suffer from low stabilization capacity of colloidal nanoparticles, which leads to lower values of accessible catalyst surface area. The current work tested the maximum possible time-invariant colloidal concentration, nanoparticle uptake, of copper oxide, by overloading the microemulsion system with excess copper oxide product. The microemulsion and operation variables which favored high uptake were identified. In addition, this study tested the applicability of a previous model developed to describe iron oxide nanoparticle uptake by the same microemulsions and provided more insight on the physical interpretation of the model parameters. The nanoparticle uptake was found to be dependent on the ionic strength of the water pools and the degree of interaction between the surfactant head groups and the stabilized nanoparticles. The water content of the microemulsions impacted the two parameters simultaneously. A time-independent concentration, uptake, was achieved after 1 h of mixing, and the colloidal nanoparticles were stable for more than two months. At constant value of R, the increase in the surfactant concentration increased the population of the reverse micelles and resulted in higher nanoparticle uptake and larger particle size. The increase of the particle size was attributed to aggregation as a result of higher probability of collision between nanoparticle-populated reverse micelles. An optimum R value corresponding to a maximum copper oxide nanoparticle uptake was obtained at R of 5.0. At relatively low R, increasing R increased the nanoparticle uptake due to the increase of the size of reverse micelle and the solubilization capacity of $CuCl_2$. Further increase in R reduced the nanoparticle uptake by decreasing the interaction between the surfactant head groups, the ionic strength of the water pools and the rigidity of the surfactant layer. Lower interaction with the stabilized nanoparticles coupled with less rigid surfactant layer promote particle aggregation and precipitation of particles with sizes exceeding the stabilization capacity of the microemulsion. The nanoparticle uptake and particle size increased as the concentration of $CuCl_2$ in the microemulsions increased. This was attributed to the increase in precursor ion occupancy number and the rigidity of surfactant layer. Higher occupancy number coupled with rigid layer promotes intramicellar nucleation and growth and contributes to higher uptake. At the same experimental conditions, AOT microemulsions can stabilize less colloidal copper oxide nanoparticles when compared with colloidal iron oxide nanoparticles. This is believed to be due to a higher interaction between AOT head groups and iron oxide nanoparticles. A mathematical model, which accurately described the nanoparticle uptake as a function of R, precursor concentration, and surfactant concentration was evaluated. The model agreed well with the experimental results. Critical evaluation of the experimental results and the model parameters further supported the higher interaction between the surfactant head groups and the stabilized iron oxide nanoparticles.

Surface areas per gram of catalyst were higher than the literature values. Higher nanoparticle uptake corresponded to higher accessible area per unit volume of the microemulsion. Nonetheless, particle aggregation at high uptake and low surfactant layer rigidity limited the surface area per unit volume of the microemulsion.

Acknowledgments

The authors thank the following organizations for the financial support: Natural Science and Engineering Research Council of Canada (NSERC), Alberta Ingenuity Centre for In Situ Energy (AICISE), Centre for Environmental Engineering Research and Education (CEERE), and Alberta Ingenuity Fund. N. Nassar gratefully acknowledges Ursula and Herbert Zandmer, and J.B. Hyne for their awards.

Supporting material

Supplementary material for this article may be found, on ScienceDirect, in the online version.

Please visit DOI: 10.1016/j.jcis.2007.08.044.

References

[1] A.D. Bianco, N. Panarit, S.D. Carlo, J. Elmouchnino, B. Fixari, P.L. Perchec, Appl. Catal. A 94 (1993) 1–16.
[2] A.D. Bianco, N. Panariti, S.D. Carlo, P.L. Beltrame, P. Carnit, Energy Fuels 8 (1994) 593–597.
[3] R.R. Anderson, B.C. Bockrath, Fuel 63 (1984) 329–333.
[4] D.E. Herrick, J.W. Tieney, I. Wender, G.P. Huffman, F.E. Huggins, Energy Fuels 4 (1990) 231–236.
[5] A. Martino, J.P. Wilcoxon, J.S. Kawola, Energy Fuels 8 (1994) 1289–1295.
[6] M. Boutonnet, J. Kizling, V. Mintsa-Eya, A. Choplin, R. Touroude, G. Maire, P.J. Stenius, J. Catal. 103 (1987) 95–104.
[7] M. Boutonnet, J. Kizling, R. Touroude, G. Maire, P. Stenius, Appl. Catal. 20 (1986) 163–177.
[8] J. Rymes, G. Ehret, L. Hilaire, M. Boutonnet, K. Jiratova, Catal. Today 75 (2002) 297–303.
[9] S. Nassos, E.E. Svensson, M. Nilsson, M. Boutonnet, S. Jaras, Appl. Catal. B 64 (2006) 96–102.
[10] J. Agrell, K. Hasselbo, K. Jansson, S.G. Jaras, M. Boutonnet, Appl. Catal. A 211 (2001) 239.
[11] M. Kishida, K. Umakoshi, J. Ishiyama, H. Nagata, K. Wakabayashi, Catal. Today 29 (1996) 355.
[12] C.W. Curtis, J.L. Pellegrino, Energy Fuels 3 (1989) 160–168.
[13] L. Shen, P.E. Laibinis, T.A. Hatton, Langmuir 15 (1999) 447–453.
[14] T. Masui, K. Fujiwara, K. Machida, G. Adachi, Chem. Mater. 9 (1997) 2197–2204.
[15] M.M. Husein, M.E. Weber, J.H. Vera, Langmuir 16 (2000) 9159–9167.
[16] K. Holmberg, Adv. Colloid Interface Sci. 51 (1994) 137–174.
[17] N. Nassar, M. Husein, Langmuir (2007), in press.
[18] Y. Hwang, J.K. Lee, C.H. Lee, Y.M. Jung, S.I. Cheong, C.G. Lee, B.C. Ku, S.P. Jang, Thermochim. Acta 455 (2007) 70–74.
[19] P. Keblinski, J.A. Eastman, D.G. Cahill, Mater. Today 8 (2005) 36–44.
[20] J.A. Eastman, S.U.S. Choi, S. Li, W. Yu, L.J. Thompson, Appl. Phys. Lett. 78 (2001) 718.
[21] M.P. Pileni, J. Phys. Chem. 97 (1993) 6961–6973.
[22] M. Husein, E. Rodil, J.H. Vera, Langmuir 22 (2006) 2264–2272.
[23] M. Husein, E. Rodil, J.H. Vera, J. Colloid Interface Sci. 288 (2005) 457–467.
[24] N. Nassar, M. Husein, Phys. Status Solidi A 203 (2006) 1324–1328.
[25] S. Hingorani, V. Pillai, P. Kumar, M.S. Multani, D.O. Shah, Mat. Res. Bull. 28 (1993) 1303–1308.
[26] M. Zulauf, H.-F. Eicke, J. Phys. Chem. 83 (1979) 480–486.
[27] M.P. Pileni, T. Zemb, C. Petit, Chem. Phys. Lett. 118 (1985) 414–420.
[28] J. Eastoe, B.H. Robinson, A.J.W.G. Visser, D.C. Steytler, J. Chem. Soc. Faraday Trans. 87 (1991) 1899–1903.
[29] F. Debuigne, L. Jeunieau, M. Wiame, J.B. Nagy, Langmuir 16 (2000) 7605–7611.
[30] B.J. Palla, D.O. Shah, P. Garcia-Casillas, J. Matutes-Aquino, J. Nanopart. Res. 1 (1999) 215–221.
[31] V. Pillai, P. Kumar, M. Hou, P. Ayyub, D. Shah, Adv. Colloid Interface Sci. 55 (1995) 241–269.
[32] M.A. Lopez-Quintela, J. Rivas, J. Colloid Interface Sci. 158 (1993) 446–451.
[33] R.P. Bagwe, K.C. Khilar, Langmuir 13 (1997) 6432–6438.
[34] R.P. Bagwe, K.C. Khilar, Langmuir 16 (2000) 905–910.
[35] P. Guering, B. Lindman, Langmuir 1 (1985) 464–468.
[36] J. Sjoblom, R. Skurtveit, J.O. Saeten, B. Gestblom, J. Colloid Interface Sci. 141 (1991) 329–337.
[37] A. Taleb, C. Petit, M.P. Pileni, Chem. Mater. 9 (1997) 950–959.
[38] H.R. Rabie, D. Helou, M.E. Webber, J.H. Vera, J. Colloid Interface Sci. 189 (1997) 208–215.
[39] H.R. Rabie, M.E. Weber, J.H. Vera, J. Colloid Interface Sci. 174 (1995) 1–9.
[40] H.R. Rabie, J.H. Vera, Fluid Phase Equilib. 122 (1996) 169–186.

Further reading

[41] M.M. Husein, E. Rodil, J.H. Vera, J. Nanopart. Res. 9 (2006) 787–796.
[42] Y. Zhao, J.-J. Zhu, J.-M. Hong, N. Bian, H.-Y. Chen, Eur. J. Inorg. Chem. (2004) 4072–4080.
[43] R.M. Cornell, U. Schwertmann, The Iron Oxides: Structure, Properties, Occurrences, and Uses, second ed., Wiley–VCH, New York, 2003.
[44] S. Mann, J.P. Hannington, J. Colloid Interface Sci. 122 (1988) 326–335.